Radiophysics and Quantum Electronics, Vol. 56, No. 2, July, 2013
(Russian Original Vol. 56, No. 2, February, 2013)

INFLUENCE NONUNIFORMITY OF THE ATMOSPHERIC WATER VAPOR FIELD ON THE PHASE MEASUREMENTS OF RADIO SIGNALS FROM GLOBAL NAVIGATION SATELLITE SYSTEMS

V. V. Kalinnikov, O. G. Khutorova, and G. M. Teptin *

UDC 537.876:551.51

We present the experimental results for the horizontal gradients of integrated content of atmospheric water vapor, which are retrieved from the phase measurements of signals in the receiver network of the global navigation satellite systems in 2011 in the Republic of Tatarstan. The seasonal gradient variation is found. The meridional gradient usually shows a decrease in integrated water vapor with increasing latitude, and its monthly mean values are equal to -1.8 *mm and* 0.1 *mm of precipitable water per* 100 *km in August and December, respectively. The zonal monthly average gradient is somewhat smaller in magnitude than the meridional one and is equal* 0.1 *mm and* -0.8 *mm per* 100 *km in March/June and May/October, respectively. Instantaneous values of the gradients can by an order of magnitude higher than the monthly mean values. Contribution from the gradient of integral water vapor to the phase-measurement difference between two antennas spaced* 30 *km apart is shown to attain its maximum of* 141.5 *mm in August for the zenith angle* 80°. *Errors in determining the mutual location of the ground-based antennas of global navigation satellite systems due to the water vapor gradients can reach* 66 *mm and* 16.9 *mm in August and February, respectively.*

1. INTRODUCTION

It is well known that the refractive index of decimeter radio waves in the atmosphere significantly depends on the dry air pressure and temperature and the water vapor pressure [1]. Radio signals of global navigation satellite systems, which are used for determining the receiving-antenna location on the Earth's surface, are subject to atmospheric refraction, which, on the one hand, reduces the accuracy of the measurement results, but, on the other hand, allows us to use the ground-based receiver networks of such systems for remote tropospheric sensing [2–5]. In the studies of this problem, the integrated water vapor, i.e., the parameter characterizing the amount of water vapor in the atmospheric column, is usually used [6]. The measurement units for this parameter are millimeters (or kilograms) of precipitable water. This value is subject to significant seasonal and meteorological variations. In addition, integrated water vapor is spatially nonuniform [6], which leads to nonuniformities of the atmospheric refractivity of radio waves.

Ground-based receiving antennas of global navigation satellite systems use radio signals transmitted by satellites for calculating the mutual locations of receivers. This problem is solved by finding the phase difference of the radio signals arriving from satellites [7]. The influence of the field of integrated water vapor on the obtained results is a function of both the horizontal gradients of this field and the length and azimuth of the baseline connecting two receiving antennas.

Using short measurement sessions (with a duration of 0.5–1 h), which are usually used in practice, it is almost impossible to estimate neither the value of integrated water vapor, nor its gradients [8]. However,

* guerman.teptin@ksu.ru

Kazan' (Volga Region) Federal University, Kazan, Russia. Translated from Izvestiya Vysshikh Uchebnykh Zavedenii, Radiofizika, Vol. 56, Nos. 2, pp. 96–103, February 2013. Original article submitted February 12, 2013; accepted February 28, 2013.

there exist continuously operating station networks of the global navigation satellite systems, which perform 24-h records of the measurement results. The data collected by such networks for 24-h and longer periods can be used for finding the desired quantities.

This work is aimed at determining the gradients of the field of integrated water vapor from the phase measurements of the High-Precision Positioning Network of the Republic of Tatarstan [9], as well as estimating the gradient-produced errors in the calculations of the mutual location of the receiver antennas.

2. DETERMINATION OF INTEGRATED WATER VAPOR BY MEASURING THE SIGNALS FROM GLOBAL NAVIGATION SATELLITE SYSTEMS

The satellites of the navigation systems emit signals at the decimeter-range carrier frequencies, i.e., approximately 1.2 and 1.5 GHz [7]. When propagating through different atmospheric layers, these signals are subject to refraction. For neutral gases, the refractivity N, which is related to the refractive index n, is written as [10]

$$N = (n-1)\cdot 10^6 = 77.6890\frac{P[\text{mbar}]}{T[\text{K}]} + 71.2952\frac{e[\text{mbar}]}{T[\text{K}]} + 375\,463\frac{e[\text{mbar}]}{(T[\text{K}])^2}, \tag{1}$$

where P is the dry air pressure, T is the air temperature, and e is the water vapor pressure.

The parameter characterizing the neutral-atmosphere influence on the satellite radio signals is usually the tropospheric zenith total delay (ZTD), which is defined as [8, 11]

$$\text{ZTD} = 10^{-6}\int\limits_{h_\text{r}}^{h_\text{s}} N(h)\,\text{d}h. \tag{2}$$

Here, h_r and h_s are the receiver and satellite altitudes, respectively. Therefore, ZTD shows the extent to which the phase-path length from the satellite to the receiver in the vertical (zenith) direction exceeds the geometric distance between them. Since the refractivity is linearly related to the dry-air and water-vapor pressures, it can be divided into two parts, one of which depends on total atmospheric pressure, while the other part is stipulated only by water vapor. Correspondingly, ZTD can also be represented as a sum of the so-called zenith hydrostatic delay (ZHD) and zenith wet delay (ZWD) [8, 11]:

$$\text{ZTD} = \text{ZHD} + \text{ZWD}. \tag{3}$$

Since the satellite radio paths are oblique, the tropospheric slant total delay (STD) with higher values is usually measured in practice. Although the relation between the slant and zenith delays is a function of the refractivity altitude profile, introduction of the mapping functions m is a good approximation [11]:

$$\text{STD} = \text{ZTD}\,m(z), \tag{4}$$

where z is the zenith angle. In the simplest case, the mapping function is the secant of the satellite zenith angle. However, such an approximation is satisfactory only for the zenith angles which do not exceed 60° [8]. To simulate the tropospheric delays for the lower directions, more complicated expressions are used. We established that for the middle latitudes of European Russia, the Mendes mapping function is the most accurate [12, 13].

The tropospheric zenith total delay can be estimated from the phase-measurement equations as follows [7, 14]:

$$\Phi = S + c\,(\text{d}t_\text{r} - \text{d}t_\text{s}) + K\lambda - I + \text{ZTD}\,m(z) + \varepsilon, \tag{5}$$

where Φ is the phase path, S is the geometric distance between the receiver and the satellite, c is the speed of light in free space, $\text{d}t_\text{r}$ is the receiver-clock error, $\text{d}t_\text{s}$ is the satellite-clock error, K is the phase ambiguity

in the cycles, λ is the carrier wavelength, I is the ionospheric phase delay of radio signals, ZTD is the tropospheric zenith total delay, $m(z)$ is the mapping function, and ε is other noise of the phase measurements. We exclude the ionospheric delay when writing a linear combination of the phase measurements which are made for the same satellite at two carrier frequencies [7, 15]. Then the double differences of Eq. (5) are composed, namely, the differences between the receiver measurements simultaneously for two satellites and then the differences for the neighbor time instants, such that the former and latter differences allow us to rule out the receiver-clock error and the phase ambiguities, respectively. To calculate the satellite–receiver path length, one should know the exact coordinates and clock errors of the satellite, which can be obtained from the data of the International Global Navigation Satellite System Service [16]. The system of equations composed of the measurements over all synchronously visible satellites is solved with respect to the zenith tropospheric delay using the Kalman filtering [17].

The obtained ZTD series are transformed to the integrated water-vapor series. If the atmospheric pressure is known, then using the Saastamoinen model, we can estimate the hydrostatic component of tropospheric delay [11]. Subtracting the hydrostatic part from the total delay, we obtain the wet component. Further transformation of the wet delay to integrated water vapor is performed by the procedure described in [8]. The examples of the time series of the total and hydrostatic delays, as well as the corresponding annual variation in integrated water vapor, which were obtained with a step of 5 min for 2011, are shown in Figs. 1 and 2. In [8, 14], it is shown that the absolute error of retrieving integrated water vapor from measurements of the signals from global navigation satellite systems is 1.5 mm.

3. CALCULATION OF THE GRADIENTS OF INTEGRATED WATER VAPOR

The integral water vapor series were calculated by measuring radio signals collected by the receivers of the High-Precision Positioning Network of the Republic of Tatarstan in 2011 [9]. The data of these receivers cover the region with a length of about 300 km along the east–west line and 100 km along the north–south line. The central network point has the coordinates 55.54°N and 50.99°E. The near-surface temperature and pressure, which are required to transform ZTD to integrated water vapor, are taken from the numerical weather fields NCEP/NCAR [18].

For the integrated water vapor values measured at each station, the following equation can be written:

$$\mathrm{IWV}(x,y) = \mathrm{IWV}(x_0,y_0) + \frac{\partial\,\mathrm{IWV}}{\partial x}(x-x_0) + \frac{\partial\,\mathrm{IWV}}{\partial y}(y-y_0), \tag{6}$$

where x and y are station coordinates in the northern and eastern directions, respectively, $\mathrm{IWV}(x,y)$ is the integrated water vapor value measured at the station, x_0 and y_0 are the coordinates of the central network point, and $\partial\,\mathrm{IWV}/\partial x$, and $\partial\,\mathrm{IWV}/\partial y$ are the meridional and zonal gradients of IWV, respectively. The equations are written for the IWV values, which are simultaneously measured at all stations, and are jointly solved by the least-square method. Therefore, the network-average gradient values and integrated water vapor are determined. The accuracy of these values is estimated by the standard deviation of residual differences.

4. RESULTS

We calculated the mean values of integrated water vapor, the mean and maximum (in magnitude) values of its horizontal gradients, and the maximum spatial standard deviations of integrated water vapor for each month of 2011. The results are shown in Table 1, according to which the atmosphere was driest and most humid in February and July, respectively. The meridional gradient in the cold period was several times smaller than that in the warm period, which is natural by virtue of small water-vapor content in the troposphere for negative temperatures. The maximum (in magnitude) value of the meridional gradient is reached in August such that the negative values show the general law of the integrated water vapor distribution, i.e., a decrease with increasing latitude. As a rule, the maximum gradients significantly exceed

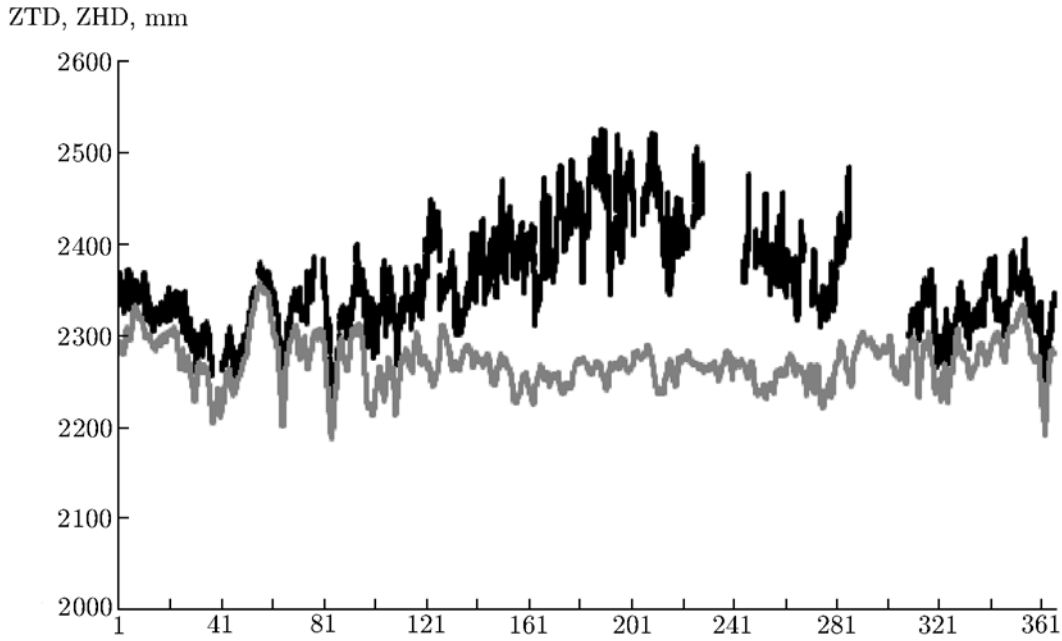

Fig. 1. Total tropospheric delay (black curve) of the satellite-system radio signals and its hydrostatic component (gray curve) for Al'met'evsk, Russia, in 2011 as a function of the day serial number.

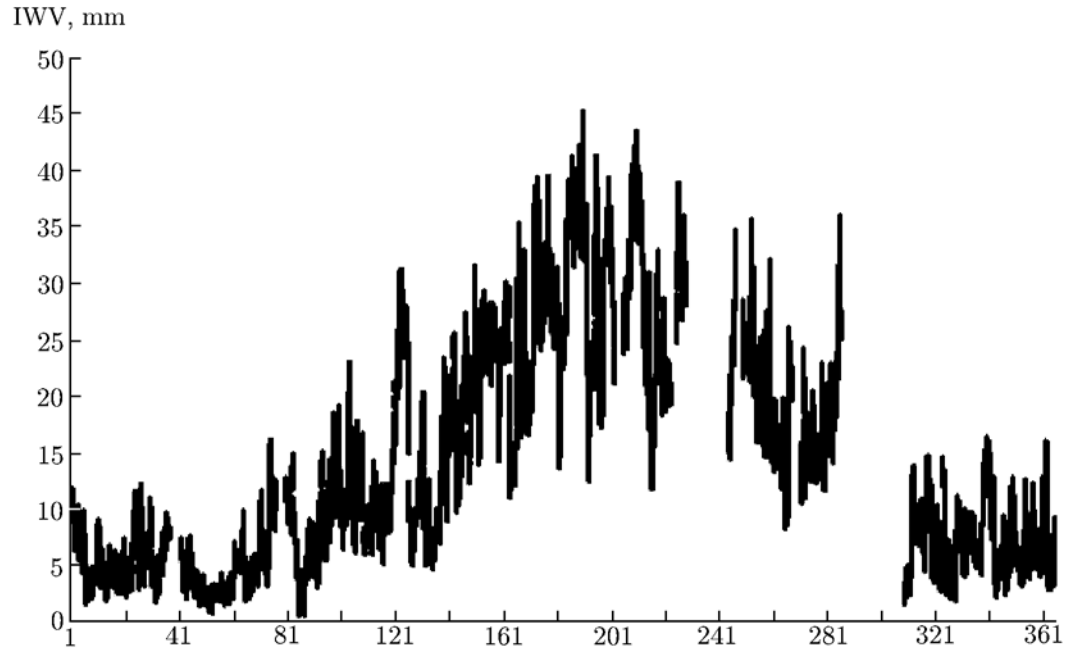

Fig. 2. Integrated water vapor IWV above Al'met'evsk, Russia, in 2011 as a function of the day serial number.

their monthly mean values. The maximum gradients are mostly observed in the period from May to August and reach 7–12 mm per 100 km. The water-vapor standard deviation above the considered region shows that the spatial fluctuations in the warm period of the year are a factor of 1.5–2 greater than those in the cold period, which corresponds to the numerical simulation results [4].

An error in determining instantaneous meridional gradients was in the interval 0.1–3.4 mm per 100 km and on the average was 0.6 mm per 100 km. For the zonal gradients, the following values were observed: 0–1.6 mm per 100 km and on the average, 0.3 mm per 100 km. In this case, the maximum and minimum

TABLE 1. The monthly mean values, monthly mean and maximum (in magnitude) horizontal gradients, and maximum spatial standard deviations of IWV.

Month	IWV(x_0, y_0), mm	σ_{IWV}, mm	$\partial\,\mathrm{IWV}/\partial x$, mm/100 km		$\partial\,\mathrm{IWV}/\partial y$, mm/100 km	
			mean value	maximum value	mean value	maximum value
1	5.9	3.5	-0.486 ± 0.006	-3.2 ± 0.3	-0.384 ± 0.003	-3.3 ± 0.2
2	4.0	1.9	-0.355 ± 0.007	-2.7 ± 0.4	-0.286 ± 0.003	-1.7 ± 0.2
3	8.3	3.4	-0.526 ± 0.012	-3.8 ± 0.6	0.122 ± 0.005	2.6 ± 0.3
4	10.9	5.3	-0.732 ± 0.008	-7.0 ± 0.6	-0.209 ± 0.004	5.1 ± 0.4
5	15.9	5.9	-1.383 ± 0.010	-8.6 ± 1.1	-0.786 ± 0.004	-5.5 ± 0.5
6	24.2	5.2	-0.927 ± 0.013	8.9 ± 1.4	0.054 ± 0.006	4.5 ± 0.6
7	26.7	3.6	-1.490 ± 0.019	-7.0 ± 1.0	-0.015 ± 0.009	2.6 ± 0.5
8	21.3	6.7	-1.760 ± 0.020	-12.5 ± 1.0	-0.229 ± 0.009	5.6 ± 0.8
9	20.0	5.4	-0.820 ± 0.010	-5.8 ± 0.7	-0.591 ± 0.005	-5.0 ± 0.5
10	18.1	4.6	0.187 ± 0.012	3.9 ± 0.5	-0.836 ± 0.005	-4.0 ± 0.7
11	7.1	4.0	-0.246 ± 0.005	-2.6 ± 0.5	-0.344 ± 0.002	-3.5 ± 0.4
12	8.3	3.5	0.100 ± 0.007	-4.0 ± 0.5	-0.740 ± 0.003	-3.4 ± 0.4

ambiguities in the gradient estimates were observed in summer and winter, respectively. The error of estimating the meridional monthly gradient varies in the range 0.005–0.020 mm per 100 km, while that of the zonal gradients varies from 0.003 to 0.009 mm per 100 km.

As was mentioned above, for the high-precision radio-engineering measurements, the influence of the field gradients of the integrated water vapor field on the difference of the phase measurements performed at the ends of the baseline is an important factor. It is obvious that this influence is maximum when the baseline is parallel to the field gradient, i.e., if its azimuth A is determined by the expression

$$\tan A = \frac{\partial\,\mathrm{IWV}}{\partial y} \Big/ \frac{\partial\,\mathrm{IWV}}{\partial x}. \tag{7}$$

In this case, the difference in the integrated water vapor values at the baseline ends is equal to

$$\Delta\mathrm{IWV} = L\sqrt{\left(\frac{\partial\,\mathrm{IWV}}{\partial x}\right)^2 + \left(\frac{\partial\,\mathrm{IWV}}{\partial y}\right)^2}, \tag{8}$$

where L is the distance between the antennas. The water vapor difference in Eq. (8) corresponds to the difference in the tropospheric zenith wet delays of the phase measurements [8, 11]:

$$\Delta\mathrm{ZWD} = \left[0.102 + \frac{1708.8}{50.4 + 0.789T[\mathrm{K}]}\right]\Delta\mathrm{IWV}, \tag{9}$$

where T is the near-ground temperature. In [11], it is shown that Eq. (9) yields satisfactory accuracy in the middle latitudes. In practice, we usually use measurements to the satellites with zenith angles not exceeding 80°, and the baseline lengths are restricted by 30 km. For such conditions, we estimated phase fluctuations and the contribution of the horizontal gradient of integrated water vapor to the difference between phase measurements of the receivers of the global navigation satellite systems. The measurements were performed at the ends of the baseline for the same satellite, and the estimates were based on Eqs. (4), (8), and (9), near-ground temperature values, and the data given in Table 1. The monthly maximum phase fluctuations and their contribution to the phase-measurement differences reached 69.6/141.5 mm and 21.5/36.3 mm in August and February, respectively. Contribution from the monthly-mean horizontal gradient of integrated

TABLE 2. Errors Δh in determining the antenna-altitude differences due to the maximum water vapor gradients on a 30-km baseline.

Month number	1	2	3	4	5	6	7	8	9	10	11	12
Δh, mm	24.2	16.9	24.0	43.4	49.7	48.3	35.4	66.0	37.4	27.9	22.8	27.1

water vapor moisture content to the phase-measurement difference amounted to 18.3 mm and 5.1 mm in August and February, respectively, which, in turn, contributes to the systematic-error formation.

In [19], it is shown that the additional difference of the phase measurements due to tropospheric delays primarily influences calculation of the difference of the antenna altitudes and the coefficient of proportionality between the errors in the altitudes and the differences in the zenith tropospheric delays is 2.59 for the middle latitudes. We calculated these errors for the maximum gradients on 30-km baselines that are aligned with the gradients. The results are given in Table 2.

It follows from Table 2 that the influence of integrated water vapor on the phase measurements of radio signals can be significant for determining the mutual location of the receiving antennas of the global navigation satellite systems. The summer trend is well pronounced, i.e., the summer errors are much greater than those in winter.

5. CONCLUSIONS

In this work, we obtained the monthly-mean horizontal gradients of the field of integrated atmospheric water vapor using the phase measurements of the signals from global navigation satellite systems, were gathered by the continuously operating station network in the Republic of Tatarstan in 2001. During the year, the meridional gradient varies approximately from -1.8 mm per 100 km (in August) to 0.1 mm per 100 km (in December), whereas the zonal gradient variation is from 0.1 mm per 100 km (in March and June) to -0.8 mm per 100 km (in May and October). For the majority of months, the meridional gradient is negative, which is indicative of a general decrease in integrated water vapor with increasing geographical latitude.

The obtained gradients significantly influence the phase-measurement differences and, thus, the determination of the mutual location of the receiving antennas of the navigation systems. The errors in calculating the mutual location can reach 66 mm and 16.9 mm in August and February, respectively. The obtained results are of interest for a wide range of problems using the high-precision measurements in the decimeter range.

We thank the Ministry for Informatization and Communications of the Republic of Tatarstan for providing access to the data of the High-Precision Positioning Network of the Republic of Tatarstan.

This work was partially supported by the Russian Foundation for Basic Research (project No. 13–05–97054).

REFERENCES

1. O. I. Yakovlev, *Space Radio Science*, Taylor and Francis, London (2003).
2. P. Haefele, L. Martin, M. Becker, et al., in: *Proc. 17th Int. Technical Meeting of the Satellite Division of the Institute of Navigation, September 21–24, 2004, Long Beach, USA*, p. 2289.
3. O. G. Khutorova, G. M. Teptin, A. A. Vasilyev, et al., *Radiophys. Quantum Electron.*, **54**, No. 1, 1 (2011).
4. G. M. Teptin, O. G. Khutorova, D. P. Zinin, et al., *Radiophys. Quantum Electron.*, **53**, No. 1, 1 (2010).
5. V. E. Khutorov, A. A. Zhuravlev, and G. M. Teptin, *Radiophys. Quantum Electron.*, **55**, No. 5, 289 (2012).

6. O. G. Khutorova, V. V. Kalinnikov, and T. R. Kurbangaliev, *Atmos. Okean. Opt.*, **25**, No. 6, 429 (2012).
7. G. Xu, *GPS: Theory, Algorithms, and Applications*, Springer, Berlin (2007).
8. T. Schuler, "On ground-based GPS tropospheric delay estimation." PhD thesis, Munchen (2001), p. 364.
9. http://85.233.70.122:8080/geopp_gnweb/gnweb.html .
10. J. M. Rueger, *Refractive Indices of Light, Infrared and Radio Waves in the Atmosphere*, UNSW, Sydney (2002).
11. V. B. Mendes, *Modeling the Neutral-Atmospheric Propagation Delay in Radiometric Space Techniques*, UNB, Brunswick (1999).
12. V. B. Mendes, G. Prates, E. C. Pavlis, et al., *Geophys. Res. Lett*, **29**, No. 10, 53 (2002).
13. V. V. Kalinnikov and G. M. Teptin, *Inzh. Izys.*, No. 5, 26 (2012).
14. V. V. Kalinnikov, O. G. Khutorova, and G. M. Teptin, *Izvestiya, Atmos. Ocean. Phys*, **48**, No. 6, 631 (2012).
15. S. Schaer, "Mapping and predicting Earth's ionosphere using the Global Positioning System." PhD thesis, Bern (1999).
16. http://igscb.jpl.nasa.gov/components/usage.html .
17. K. Brammer and G. Siffling, *Kalman–Bucy Filters*, Artech House, Norwood, Ma. (1989).
18. E. Kalnay, M. Kanamitsu, R. Kistler, et al., *Bull. Am. Meteor. Soc.*, **77**, No. 3, 437 (2011).
19. R. Santerre, *GPS Satellite Sky Distribution: Impact on the Propagation of Some Important Errors in Precise Relative Positioning*, UNB, Brunswick (1989).